Published June 24, 2014

Journal of Environmental Quality TECHNICAL REPORTS
ATMOSPHERIC POLLUTANTS AND TRACE GASES

Speciation and Isotopic Composition of Sulfur in Limestone Soil and Yellow Soil in Karst Areas of Southwest China: Implications of Different Responses to Acid Deposition

Wei Zhang,* Cong-Qiang Liu, Zhong-Liang Wang, Li-Li Zhang, and Xu-Qiang Luo

The contents and stable S isotope ratio ($\delta^{34}S$) values of total S, organic S, SO_4^{2-}–S, and total reduced inorganic S (TRS) in typical limestone soil and yellow soil were analyzed in this study to examine the general distributions of S forms and their $\delta^{34}S$ values in soils in karst areas of southwest China. Under a similar level of acid deposition, the vertical profiles of the S forms and their $\delta^{34}S$ values differed in limesto\ne soil and yellow soil, indicating the different geochemical responses of these soils to acid deposition. The deposited SO_4^{2-} was retained as organic S in both soils. The depletion in ^{34}S of TRS relative to SO_4^{2-} and the parallel increasing $\delta^{34}S$ values of TRS and SO_4^{2-} indicate a bacterial reduction process of sulfate in both soils. The different extents of C-bonded S mineralization and organic sulfate transport explain the different vertical profiles of total S and organic S contents in both soils. Sulfate adsorption in limestone soil was negligible because of high pH values. Sulfate adsorption in yellow soil was another important S retention process in addition to biological S retention to form organic S and TRS because of low pH values. The effect of acid deposition on yellow soil appeared more serious because of the accumulation and leaching of deposited SO_4^{2-}, which can result in soil acidification and accelerate the loss of basic cations from yellow soil. However, compared with yellow soil, limestone soil released more S into rivers by organic S mineralization after a large decrease in annual S deposition rate.

Karst areas in and around Guizhou Province in southwestern China are at the center of the Southeast Asian karst region, where the continuous outcrop area of carbonate rocks is the largest worldwide and where karstification is most developed (Xu and Liu, 2007). Karst areas in southwest China have been suffering from serious acid deposition since the 1970s (Zhao and Sun, 1986; Zhao et al., 1988). The acid deposition in southwest China exhibits a typical "sulfuric acid" pattern (Wang et al., 2011). Due to the predominant use of S-rich coal, the pollutant sulfur (S) is emitted mostly from widespread coal-fired power plants and home-heating activities in this region (Larssen et al., 1999, 2006, 2011). Recent data from monitoring sites in southwest China show an S deposition rate ranging from ~20 to ~160 kg S ha^{-1} yr^{-1}, a range that is higher than that of the "Black Triangle" area in Central Europe reported in the early 1980s (Larssen et al., 2006).

Long-term S deposition can cause accumulation of excess S in soils and may thus stimulate sulfate (SO_4^{2-}) reduction and increase the organic S content by increasing the assimilation of deposited SO_4^{2-} by plants and soil microorganisms (Alewell and Novák, 2001; Likens et al., 2002). Conversely, SO_4^{2-} leaching may be more intensive in soils under S deposition condition, which may be accompanied by increased output of SO_4^{2-} via stream water for a long period (Mitchell et al., 1996; Driscoll et al., 1998; Mörth et al., 2005). This leaching can accelerate the depletion of basic nutrient cations from soils and soil acidification (Kirchner and Lydersen, 1995; Driscoll et al., 2003). This phenomenon can degrade the quality of soil and vegetation, affect the evolution of river water chemistry, and aggravate the frailty of the ecological environment in karst areas of southwest China. Since the beginning of the 1990s, significant studies on acid deposition have been conducted from the macroscale perspective of pollution pattern, comprehensive monitoring, and control strategy of atmospheric S deposition in certain karst catchments in this region (e.g., Zhao et al., 1994; Seip et al., 1995). Other studies recently reported the effects of

J. Environ. Qual. 43:809–819 (2014)
doi:10.2134/jeq2013.09.0359
Received 11 Sept. 2013.
*Corresponding author (zhangwei8086@gmail.com).

W. Zhang and X.-Q. Luo, School of Geography and Tourism, Guizhou Normal College, Gaoxin Road No. 115 Wudang District Guiyang 550018, China; C.-Q. Liu and Z.-L. Wang, Tianjin Key Laboratory of Water Resources and Environment, Tianjin Normal Univ., Binshuixidao Road No. 393 Xiqing District Tianjin 300387, China; C.-Q. Liu and L.-L. Zhang, State Key Laboratory of Environmental Geochemistry, Institute of Geochemistry, Chinese Academy of Sciences, Guanshui Road No. 42 Nanming District Guiyang 550002, China. Assigned to Associate Editor Scott Young.

Abbreviations: AVS, acid volatile sulfide; DSR, dissimilatory sulfate reduction; TRS, total reduced inorganic sulfur.

atmospheric S deposition on the chemical composition of soil and river water (focused mainly on soil acidification, aluminum remobilization, and increasing SO_4^{2-} concentration in river water) (e.g., Larssen et al., 1998; Zhao et al., 2001; Han and Liu, 2004; Li et al., 2008). However, to our knowledge, previous studies have focused mainly on the biogeochemical processes of S in soils; studies on their environmental implications in karst areas of southwestern China remain limited.

The two major soil types in the karst areas of southwest China are limestone soil and zonal yellow soil (following the Chinese soil classification). The parent materials of limestone soil are carbonate rocks, whereas those of yellow soil are numerous. Carbonate rocks, sandstone, shale, basalt, and clayish old weathering crust can form yellow soil under warm and humid subtropical climates (Liu, 2009). In this study, the yellow soil profiles formed by carbonate rock weathering were selected for comparison with limestone soil profiles. Following the United States soil classification system, limestone soil and yellow soil may be classified as mollisols and ultisols, respectively. The age of soil formation and some basic properties of limestone soil and yellow soil differ. Limestone soil is formed during the early stage of soil formation by carbonate rock weathering, whereas yellow soil is formed during the later stage of soil formation by carbonate rock weathering (Liu, 2009). Limestone soil profiles have high organic C (3–15 wt.%) and low clay mineral (10–30 wt.%) contents, whereas yellow soil profiles have low organic C (2–7 wt.%) and high clay mineral (25–45 wt.%) contents. The pH value in the soil solution of limestone soil is approximately 7 throughout the soil profiles, whereas that of yellow soil is approximately 5 and decreases with soil depth. The content ratio of organic C to total S (C/S ratio) of limestone soil is 70–130, which is higher than that of yellow soil, which is 45–90. Decades of S deposition may result in the accumulation of different S forms in limestone soil and yellow soil. The geochemical behavior (e.g., SO_4^{2-} adsorption, bacterial dissimilatory SO_4^{2-} reduction [DSR], and organic S mineralization) may vary also because of the different basic properties of the soils (Wang et al., 2011). Studies that focus on the comparison of the geochemical behavior of S in limestone soil and yellow soil must be conducted to understand further the biogeochemical processes of S in soils and their environmental effects in karst areas of southwest China.

Analyses of inorganic and organic S forms are prerequisites to studying the biogeochemistry of S in soils. The stable S isotope ratio ($\delta^{34}S$), which is mainly controlled by the sources and transformation of S forms, is a powerful tool in tracing the geochemical processes of S in soils (Gebauer et al., 1994; Mayer et al., 1995a, 1995b; Alewell and Gehre, 1999; Zhao et al., 2003; Mörth et al., 2005; Novák et al., 2000, 2005). In this study, limestone soil and yellow soil were used as representative soil samples of karst areas in southwest China to analyze the contents and $\delta^{34}S$ values of total S, organic S, sulfate S (SO_4^{2-}–S), and total reduced inorganic S (TRS) (including elemental S, acid volatile sulfide [AVS], and iron sulfide [FeS_2]) in soils. This research investigated the general distributions of S forms and $\delta^{34}S$ values and compared the geochemical responses of S in limestone soil and yellow soil to acid depositions.

Materials and Methods

Sampling Sites

The sampling sites are in Puding County in Guizhou Province and Huanjiang County in Guangxi Zhuang Autonomous Region, China (Fig. 1). Puding and Huanjiang are typical karst areas of southwest China; two observation and research stations for the karst ecosystem were established by the Chinese Academy of Sciences in Huanjiang County in 2000 and in Puding County in 2012. The two counties have a population of <900,000 in a total area of 5663 km^2. Small coal pits are randomly distributed in the studied areas, and no big mining sites and coal-fired power industries are located in the areas. The economy in the studied areas is under developed. Pollutant S in the studied areas mostly originates by atmospheric transport from S emission from large coal-fired power plants nearby and from local home heating activities. A climate of subtropical monsoon with high humidity characterizes the two areas. The annual mean temperatures in Puding and Huanjiang are 15.6 and 17.9°C, respectively. Annual mean precipitation is 1396 mm in Puding and 1389 mm in Huanjiang. April to September is the wet season in the two areas; the precipitation in the wet season accounts for 70 to 80% of total annual precipitation. Generally, a large proportion of precipitation occurs from May to July (frequently >230 mm monthly) (Zhang, 2008; Ding, 2010). The two areas are typical karst landforms characterized by rocky slopes with different degrees of vegetation coverage. Carbonate rocks are the only

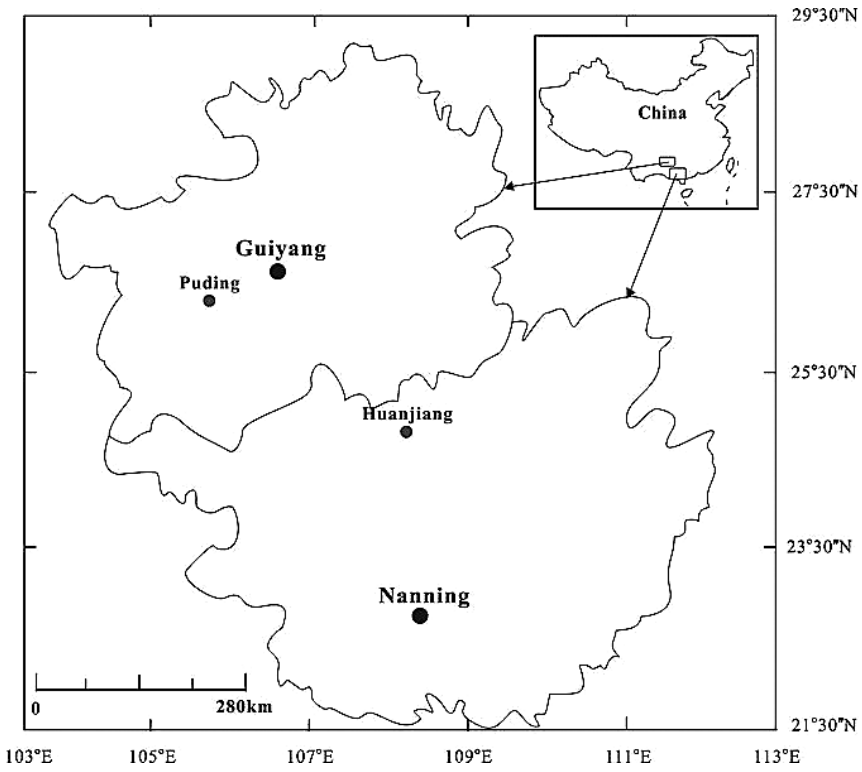

Fig. 1. Location of the study areas in Puding and Huanjiang counties, southwest China.

outcropping rocks. The soils in the two areas are mainly limestone soil and yellow soil (Fig. 2), which together account for more than 80% (limestone soil covers ~52% and yellow soil covers ~31%) of the soil area of the two counties and are representative of a large area in southwest China.

Samples of limestone soil and yellow soil were collected from two slopes in a small catchment (26°16′5.4″ N, 105°46′35.5″ E; 1358–1408 m asl) at the Puding site and from two slopes in a small catchment (24°44′32.0″ N, 108°19′27.4″ E; 353–407 m asl) at the Huanjiang site. The slopes were selected because they are practically undisturbed by land-use activities. The organic layer is thin, and the soil depth on the slopes is usually <60 cm. The dominant plant species at the Puding site are C_3 shrubs and dwarf forests, with approximately 70% coverage; C_4 herbaceous plants mixed with C_3 shrubs grow at the Huanjiang site, with approximately 60% coverage. The field descriptions of the soil sampling sites are summarized in Table 1.

Sample Collection

The bulk deposition in each of the two small catchments was monitored monthly beginning on 1 Jan. 2008 and ending on 31 Dec. 2008. The sampler was a polyethylene funnel (122 cm^2) fitted to a 1-L polyethylene bottle placed 120 cm above the ground. Three samplers were installed approximately 5 m apart in a clearing on each slope and used to sample bulk deposition. A single composite sample was prepared for analysis by combining the three samples. Soil samples were collected in late May 2008. The soil profile samples of limestone soil and yellow soil were collected from the upper, middle, and lower slopes of the selected sites. For comparison at the same sampling site, samples of limestone soil in Puding, yellow soil in Puding, limestone soil in Huanjiang, and yellow soil in Huanjiang were collected. The specific descriptions of the soil samples are shown in Table 1. Soil profile samples were obtained from the walls of the soil pits at 10-cm increments to include the entire soil thickness (usually ≤50 cm). At Puding and Huanjiang, the carbonate bedrocks (mainly detrital limestone mixed with calcareous dolomite) at the bottom of the sampled soil profiles were collected.

Sample Analyses

Soil Organic Carbon Content, Clay Content, pH Values, and Soil Water Content

Soil organic C content was measured with a PE2400 element analyzer (PerkinElmer) after acid treatment of the soil samples (Midwood and Boutton, 1998). The analytical precision was ≤0.1%. Soil clay content was determined by the pipette method (Conway, 1978). Soil pH values were measured with a glass electrode in a 1:2.5 soil–deionized water suspension (Zhu and Liu, 2006). Soil subsamples were oven-dried at 105°C to a constant weight, and the decreased weight of the subsamples after oven-drying was used to calculate the soil water content (Likens et al., 2002).

Fig. 2. Representative soil profiles at Puding and Huanjiang sites in southwest China. (a) Limestone soil. (b) Yellow soil.

Sulfur Forms and $\delta^{34}S$ Values

The total S in soils was extracted from the homogenized subsamples (<100 mesh) by digestion with an Eschka mixture (Sigma) at 800°C for 90 min in a muffle furnace and precipitated as barium sulfate ($BaSO_4$) (Novák et al., 1994). The resulting $BaSO_4$ was used to calculate the total S contents gravimetrically and was then converted to SO_2 to measure the $\delta^{34}S$ value of the total S in the soils (Alewell and Novák, 2001). Sulfate in the soils was extracted with 16 mmol L^{-1} KH_2PO_4 (Prietzel et al., 1995). The extracted liquid was filtered, and the SO_4^{2-} concentration in the filtrate was determined by routine DIONEX ICS-90 ion chromatography. Subsequently, SO_4^{2-} in the filtrate was precipitated as $BaSO_4$ by adding a $BaCl_2$ solution; the resulting $BaSO_4$ was used to measure the $\delta^{34}S$ value of SO_4^{2-} (Mayer et al., 1995a).

Considering the possible low contents of element S and AVS, the single-step distillation procedure for TRS extraction was used in the studied soils. This procedure provides a simpler and more accurate method for extracting TRS (Fossing and Jørgensen, 1989; Bates et al., 1993). After SO_4^{2-} extraction, the weighed homogenized subsamples were anaerobically treated with HCl-$CrCl_2$ solution in a modified Johnson–Nishita apparatus, by which AVS (mainly FeS) and chromium reducible S (element S+FeS_2) were quantitatively converted to H_2S. The generated H_2S was carried by N_2 gas into a zinc acetate solution to be precipitated as ZnS. The TRS content was then quantified

Table 1. Field descriptions of the studied soil profiles.

Sampling sites	Soil types	Dominant species	Positions	Slope gradient	Soil profiles
Puding	limestone soil (PL)	shrubs (e.g., *Pyracantha fortureana*, *Pubescens*, *Cyclosorus acuminatus*)	upper slope	33.1°	PL-1
			middle slope	31.4°	PL-2
			lower slope	28.2°	PL-3
	yellow soil (PY)	dwarf forest (e.g., *Pinus massoniana*, *Betula luminifera*, *Aralia chinensis*)	upper slope	38.7°	PY-1
			middle slope	34.2°	PY-2
			lower slope	25.3°	PY-3
Uanjiang	limestone soil (HL)	sparse grass (e.g., *Carex* sp., *C. acuminatus*)	upper slope	37.5°	HL-1
			lower slope	37.5°	HL-2
	yellow soil (HY)	shrubs (e.g., *C. acuminatus*, *Pubescens*)	upper slope	33.3°	HY-1
			lower slope	27.3°	HY-2

by iodometric titration (APHA, 1998). To analyze the $\delta^{34}S$ values of TRS, the resulting ZnS in the adsorption bottle was reprecipitated as silver sulfide (Ag_2S) by adding additional 10% $AgNO_3$ solution (Hall et al., 1988). The precipitated Ag_2S was filtered, washed with deionized water, and then used to measure the $\delta^{34}S$ value of TRS (Backlund et al., 2005). Organic S content was calculated by subtracting SO_4^{2-}–S and TRS content from the total S content. The $\delta^{34}S$ value of organic S in the residual subsamples was determined by applying the same Eschka digestion method for total S extraction (Bates et al., 1993). The bedrock samples were ground to pass through a 200-mesh screen. The same Eschka digestion method for total S extraction was applied to measure the S content and the $\delta^{34}S$ value of the bedrock samples.

The S blank in the Eschka mixture (Sigma) was measured with the same Eschka digestion method for total S extraction. The S content in the Eschka mixture was <0.0005 wt.% (n = 6). The normal recoveries for each S form were ≥93.0% as determined by standard addition. The $\delta^{34}S$ values of total S, organic S, SO_4^{2-}–S, and TRS in the soils were measured by continuous flow isotope ratio mass spectrometry (Giesemann et al., 1994). The overall reproducibility of stable S isotope determinations (n = 6), including the extraction of S forms, preparation of $BaSO_4$ and Ag_2S, gas preparations, and mass spectrometry measurement, was approximately ±0.5, 0.7, 0.6, 0.9, and 0.4‰ for total S, SO_4^{2-}–S, TRS, organic S, and bedrock S, respectively. The isotopic results are reported with reference to the Canyon Diablo Troilite (‰ CDT).

Results and Discussion

Soil Organic Carbon Contents, Clay Contents, C/S Ratios, pH Values, and Soil Water Contents

The vertical profiles of soil organic C contents, C/S ratios, clay contents, pH values, and soil water contents in limestone soil and yellow soil were different (Fig. 3); this result indicates differences in the basic properties of limestone soil and yellow soil. Limestone soil had relatively high organic C contents (2.6–7.1 wt.%), C/S ratios (83.7–123.7), and pH values (7.1–7.7) (Fig. 3a–c), whereas the corresponding data in yellow soil were organic C content, 1.6 to 4.9 wt.%; C/S ratios, 47.0–83.1; and pH 4.8 to 5.5. The C/S ratios decreased with increasing depth in both soil profiles. The pH values increased slightly with increasing depth in the limestone soil profiles but decreased in the yellow soil profiles. The clay content was 28.5 to 42.0 wt.% in the yellow soil profiles, which was higher than that in the limestone soil profiles (16.8–22.3 wt.%) (Fig. 3d). Clay exhibited enrichment from the surface to the bottom layers in the yellow soil profiles. The yellow soil profiles were relatively high in soil water contents (30.4–42.3 wt.%), whereas the corresponding data were 18.7 to 28.2 wt.% in the limestone soil profiles (Fig. 3e).

Sulfur Deposition and Accumulation of Sulfur Forms

During the 1-yr monitoring period, the annual volume-weighted average pH values of the bulk deposition were 4.8 in the Puding site and 4.9 in the Huanjiang site, both of which had typical acidic values. The wet deposition flux of atmospheric SO_4^{2-} was estimated to be approximately 60.6 and 50.5 kg S ha^{-1} yr^{-1} in the Puding and Huanjiang sites, respectively. The dry deposition of SO_2 was not monitored but was estimated to be of similar size to the wet deposition of SO_4^{2-} in each site, according to Zhao et al. (2001) and Larssen et al. (2006). The $\delta^{34}S$ values of deposited SO_4^{2-} varied from −3.2 to 0.8‰ and were −1.7 ± 0.9‰ (mean ± SD) in the Puding site, whereas the $\delta^{34}S$ values varied from −8.3 to −3.2‰ and were −5.4 ± 1.8‰ in the Huanjiang site.

As expected, the long-term acid deposition in the southwestern karst areas of China significantly increased the total S content of limestone soil and yellow soil (Zhou et al., 1999; Wang et al., 2011). However, under similar acid deposition conditions, the accumulation of S forms varied in both soils (Fig. 4). Organic S was the dominant S form at all depths in the limestone soil and yellow soil profiles, a result that is in agreement with that of previous studies associated with soil S forms from other sites (e.g., Mitchell et al., 1992; Stanko-Golden et al., 1994; Novák et al., 2003). However, the total S and organic S contents were generally higher in limestone soil than in yellow soil. The percentage of organic S in total S was higher in limestone soil, with organic S ranging from 78.1 to 92.9% of total S compared with a range of 74.4 to 87.2% in yellow soil.

Generally, TRS was the dominant inorganic S form in both soils; however, the TRS contents (27.1–67.7 mg kg^{-1}) were higher in yellow soil than in limestone soil (18.0–38.8 mg kg^{-1}). Meanwhile, the percentage of TRS in total S was relatively high in yellow soil, ranging from 6.5 to 15.9% of total S, compared with a range of 3.1 to 11.0% in limestone soil. The SO_4^{2-}–S con-

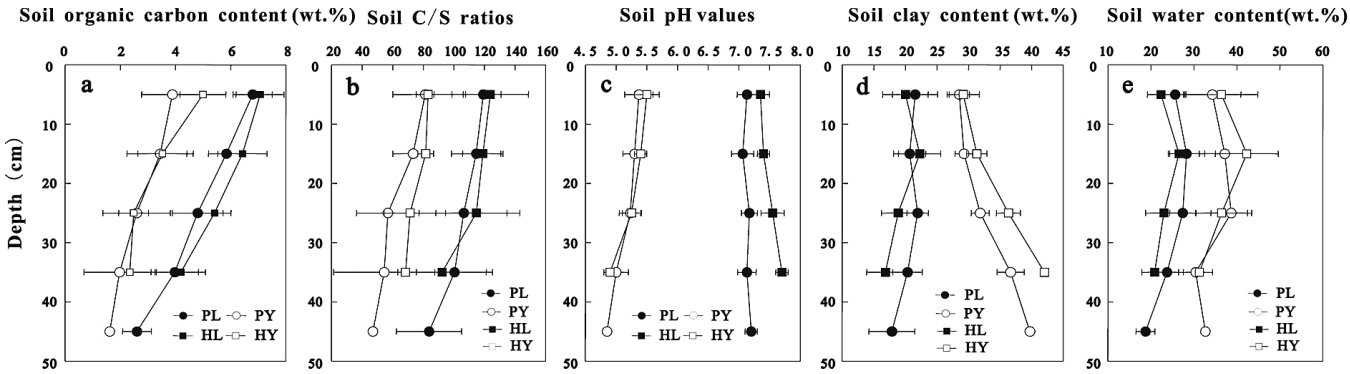

Fig. 3. Changes in soil organic C content, C/S ratios, pH values, clay content, and soil water content with depth increments in the soil profiles. Each point is the mean value of a composite of field samples at the same depths of the same soil type in the same site. Error bars represent 1 SD of the mean and provide an estimate of sample heterogeneity and analytical errors. HL, limestone soil in Huanjiang; HY, yellow soil in Huanjiang; PL, limestone soil in Puding; PY, yellow soil in Puding.

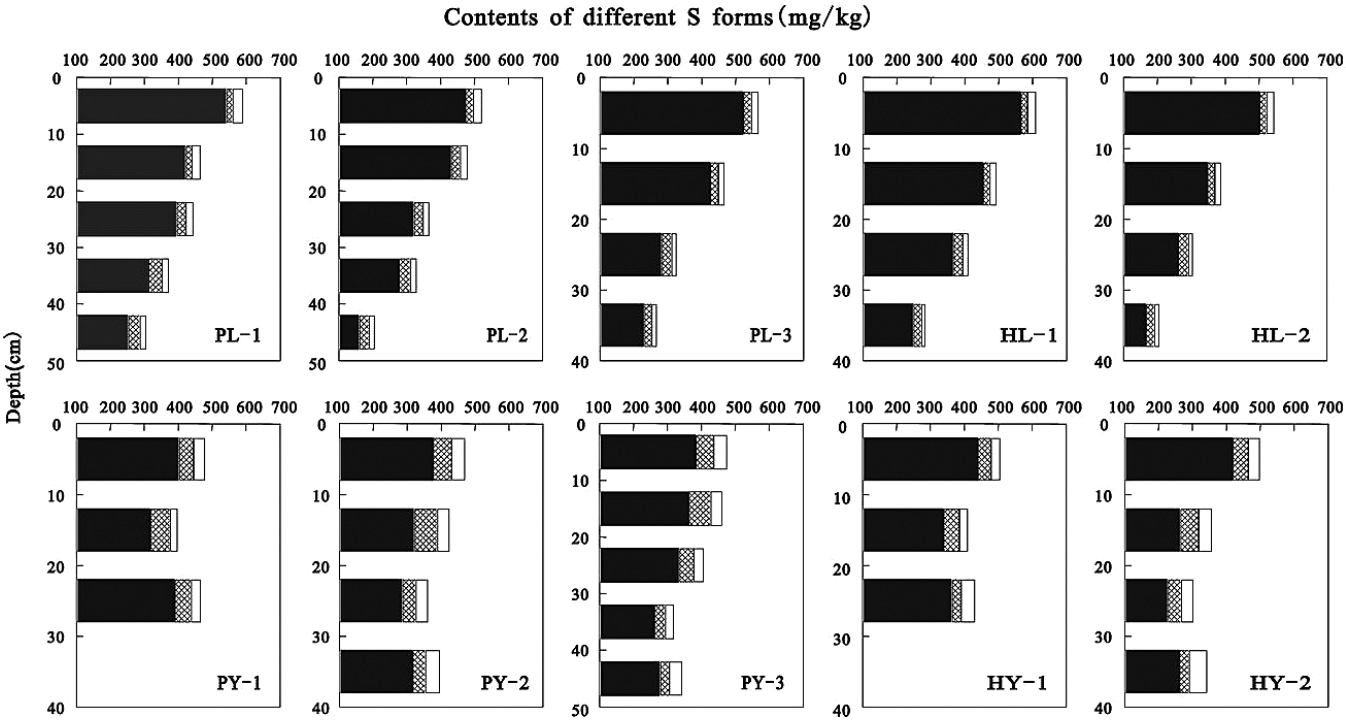

Fig. 4. Changes in S contents of total S, organic S, total reduced inorganic S (TRS), and SO_4^{2-}–S with depth in soil profiles. Black: organic S; hatched: TRS; and white: SO_4^{2-}–S. Total S is the sum of organic S, TRS, and SO_4^{2-}–S. HL, limestone soil in Huanjiang; HY, yellow soil in Huanjiang; PL, limestone soil in Puding; PY, yellow soil in Puding.

tents were 24.3 to 58.9 mg kg^{-1} in yellow soil, compared with 11.8–32.9 mg kg^{-1} in limestone soil. The relatively high SO_4^{2-}–S content in yellow soil was expected because the low pH values of yellow soil favored SO_4^{2-} adsorption (Prietzel et al., 2004).

Formation and Mineralization of Organic Sulfur

Sulfate is the dominant S form in soils that can be assimilated by plants and soil microorganisms to form organic S compounds (Likens et al., 2002). The assimilatory uptake of SO_4^{2-} by plants and soil microorganisms to form organic S compounds exhibited no significant S isotope fractionation (Krouse and Grinenko, 1991; Novák et al., 2001). Therefore, the $\delta^{34}S$ values of the organic S compounds were close to the $\delta^{34}S$ values of SO_4^{2-} at the surface layers of the studied soil profiles (Fig. 5).

Generally, the total S and organic S contents decreased, whereas the $\delta^{34}S$ values of total S and organic S increased, with soil depth in the limestone soil and yellow soil profiles (Fig. 4 and 5). This result may be explained by the continuous mineralization of organic S in the studied soils (Novák et al., 1996). Organic S mineralization is an important soil process that occurs simultaneously with organic S formation and explains the reduction of organic S contents with the increase in depth in most soil profiles (Stevenson and Cole, 1999; Lavelle and Spain, 2003). Norman et al. (2002) used an incubation–extraction experiment with Black Forest soil and showed that organic S mineralization involves a two-step reaction. The first and gradual step is the conversion of C-bonded S to organic sulfate; the residual C-bonded S fractions are enriched in ^{34}S relative to the resultant organic sulfate. The second step is the rapid hydrolysis of organic sulfate to inorganic SO_4^{2-} (also referred to as secondary SO_4^{2-}); the residual organic sulfate fractions are depleted in ^{34}S relative to the secondary SO_4^{2-}. Secondary SO_4^{2-} can then be transported downward by leaching in the soil profiles. The residual organic sulfate after hydrolyzation was labile and could be transported with soil seepage water (Schoenau and Bettany, 1987; Gebauer et al., 1994; Mitchell et al., 2001; Norman et al., 2002). Researchers generally agree that the continuously increasing $\delta^{34}S$ value of total S in soils is caused by the aging of organic S, especially by the removal of isotopically light organic sulfate–S produced by mineralization of C-bonded S (Novák et al., 2005 and references therein). In this study, the ongoing mineralization of organic S (mainly C-bonded S) resulted in the total S and organic S fractions generally being enriched in ^{34}S as depth increased in the studied soil profiles (Fig. 5).

The total S and organic S contents and the percentage of organic S in total S were higher in limestone soil than in yellow soil. This finding may be related to the smaller extent of organic S mineralization in limestone soil (Norman et al., 2002), which in turn may be related to different soil-forming processes of limestone soil and yellow soil. Limestone soil is formed during the early stage of soil formation by carbonate rock weathering and consequently undergoes a relatively short period of organic matter mineralization and basic cation leaching (Liu, 2009). Therefore, the organic matter and basic cation (e.g., Ca^{2+}, Mg^{2+}) contents are relatively high in limestone soil. Moreover, the humus produced by organic matter decomposition can combine with Ca^{2+} to form stable humus calcium in limestone soil that is slow to decompose (Bollag and Stotzky, 1990). Thus, the organic S fractions stored in the organic matter were relatively stable and exhibited less mineralization in limestone soil.

Yellow soil is formed during the later stage of soil formation by carbonate rock weathering and thus undergoes long-term organic matter mineralization and a strong leaching process, wherein basic cations (e.g., Ca^{2+} and Mg^{2+}) are leached (Liu,

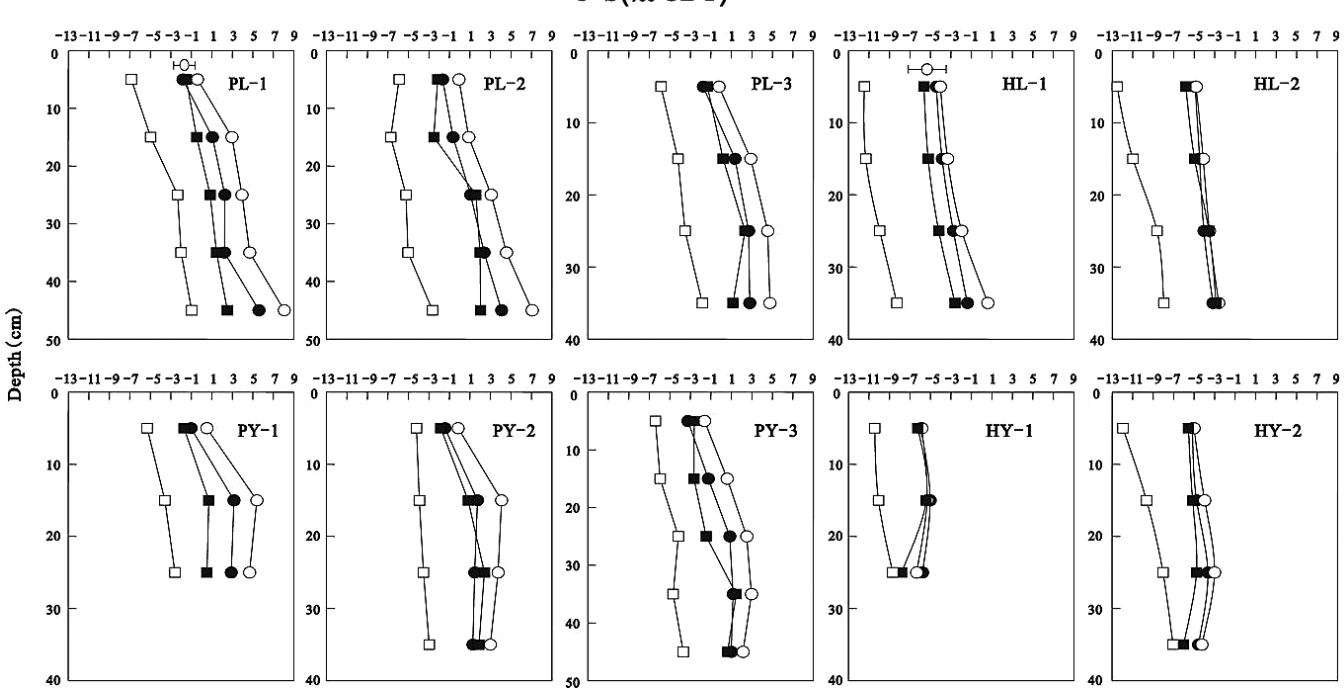

Fig. 5. Changes in $\delta^{34}S$ values of total S, organic S, total reduced inorganic S (TRS), and SO_4^{2-}–S with depth in soil profiles. Solid circle: total S; open circle: organic S; solid square: SO_4^{2-}–S; open square: TRS; and open circle with error bar: bulk deposition. HL, limestone soil in Huanjiang; HY, yellow soil in Huanjiang; PL, limestone soil in Puding; PY, yellow soil in Puding.

2009). Therefore, the organic matter content, C/S ratios, and basic cation contents are low in yellow soil. Studies on the 60-cm-deep soil profiles in the karst areas of southwestern China have shown that the average $\delta^{13}C$ values of soil organic C ($\delta^{13}C_{soc}$) increase from −25.6 to −22.4‰ with depth in the yellow soil profiles. The value of $\delta^{13}C_{soc}$ increased from −22.9‰ at the surface layers to −21.8‰ at approximately 25 cm depth and then remained unchanged below 25 cm depth in the limestone soil profiles (Li et al., 2012). On the basis of the large magnitude of $\delta^{13}C_{soc}$ fractionation in yellow soil relative to that in limestone soil, Li et al. (2012) concluded that yellow soil has a greater extent of organic matter mineralization compared with limestone soil. This mechanism may result in a larger extent of organic S mineralization in yellow soil, which could explain the lower total S and organic S contents and lower percentage of organic S in total S in yellow soil than in limestone soil.

Transport of Organic Sulfur Fraction

The depth relationship between S contents and the $\delta^{34}S$ values of organic S is shown in Fig. 6. Decreasing organic S contents and increasing $\delta^{34}S$ values of organic S with depth were observed in the limestone soil profiles; the same trends were observed at depths from the surface to the middle layers in the yellow soil profiles. Organic S contents increased below the middle layers of the yellow soil profiles, whereas the $\delta^{34}S$ values of organic S sharply decreased. This contrast may be explained by the different amounts of transported organic S fractions in limestone soil and yellow soil. The small extent of organic S (mainly C-bonded S) mineralization in the limestone soil profiles may result in a relatively small amount of transported organic sulfate. The majority of the transported organic sulfate can be hydrolyzed to secondary SO_4^{2-} and then lost by leaching without adsorption because of the high pH values in limestone soil. Therefore, the ongoing organic S mineralization and the subsequent transport and hydrolyzation of organic sulfate explain the gradual decrease in organic S contents and the increase in the $\delta^{34}S$ values of organic S with depth in the limestone soil profiles.

Yellow soils have a relatively large extent of organic S mineralization and, consequently, a large amount of organic sulfate mineralized from C-bonded S. The leaching of organic sulfate was strong in the acidic soils; this condition resulted in greater transport of organic sulfate (e.g., Tan et al., 1994; Prietzel et al., 2004). The organic sulfate from mineralization of C-bonded S has lower $\delta^{34}S$ values than the residual C-bonded S (Norman et al., 2002). On the basis of the above analyses, a reasonable explanation for the increase in organic S contents and the decrease in $\delta^{34}S$ values of organic S at the bottom layers of the yellow soil profiles was the transport and incomplete hydrolyzation of a large amount of organic sulfate under strong leaching conditions. This phenomenon resulted in the increase in total S contents and the decrease in $\delta^{34}S$ values of total S at the bottom layers in the yellow soil profiles (Fig. 4–6).

Dissimilatory Sulfate Reduction and Total Reduced Inorganic Sulfur Formation

Values of $\delta^{34}S$ for SO_4^{2-}–S on the surface layers of the soil profiles were close to the $\delta^{34}S$ values of atmospheric deposition at each site (Fig. 5). This result indicates that atmospheric deposition was the main S source of SO_4^{2-} on the surface soils of the studied soil profiles from both sites. After the biological assimilation of SO_4^{2-} to form organic S, the deposited SO_4^{2-} may undergo bacterial DSR conducted by anaerobic sulfate-reducing microorganisms to form TRS in limestone soil and yellow soil profiles (Fossing and Jørgensen, 1989; Krouse and Grinenko,

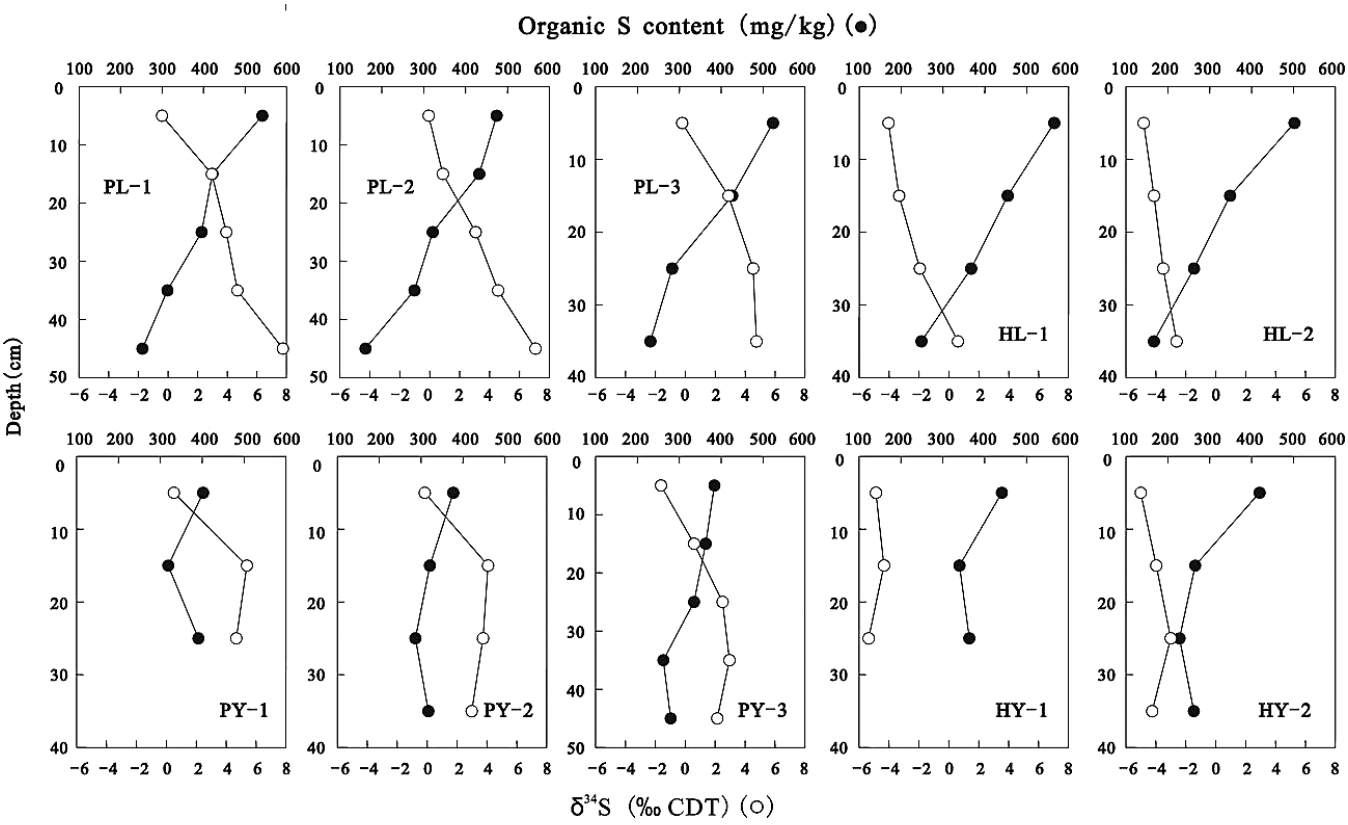

Fig. 6. Changes in S contents and $\delta^{34}S$ values of organic S with depth in soil profiles. CDT, Canyon Diablo Troilite; HL, limestone soil in Huanjiang; HY, yellow soil in Huanjiang; PL, limestone soil in Puding; PY, yellow soil in Puding.

1991). The resulting TRS product during the DSR process is significantly depleted in ^{34}S compared with the residual SO_4^{2-} (Krouse and Grinenko, 1991). As DSR continues, the $\delta^{34}S$ values of SO_4^{2-} and the resulting TRS gradually increase (Tuttle et al., 1990; Krouse and Grinenko, 1991).

In this study, the $\delta^{34}S$ values of TRS ranged from −6.8 to −0.9‰ in all soil profiles in the Puding site and from −12.5 to −7.1‰ in all soil profiles in the Huanjiang site (Fig. 5). The vertical profiles of the S contents and the $\delta^{34}S$ values of SO_4^{2-}–S and TRS in both soil types are compared in Fig. 7 and 8, respectively. Figures 5, 7, and 8 show that TRS had the lowest $\delta^{34}S$ values compared with the $\delta^{34}S$ values of other S forms in the studied soils. The SO_4^{2-}–S contents decreased with the increase in soil depth, whereas the TRS contents and the $\delta^{34}S$ values of residual SO_4^{2-} and the resulting TRS gradually increased. These results indicate that DSR continued under suitable anaerobic conditions as soil depth increased and that TRS was the main product during DSR. Under S deposition conditions, the soils of karst areas in southwest China can be considered an open system, where fresh SO_4^{2-} (from atmospheric deposition) replaces the reduced SO_4^{2-}. With the continuous input, ongoing DSR process, and the leaching of deposited SO_4^{2-}, the differences in the $\delta^{34}S$ values of SO_4^{2-} and TRS may change slightly with the increase in soil depth. This condition explains the trend of parallel increase in the $\delta^{34}S$ values of SO_4^{2-} and TRS with depth in the soil profiles (Fig. 5).

The presumably oxidized conditions in the soils did not inhibit the occurrence of DSR for the following possible reasons. The soil samples from the two areas were collected in late May, which is during the wet season (Apr.–Sept.). Wet weather dominated in the two areas in May. The sampling depths of the surface layers of the soil profiles were approximately 5 cm from the soil surface. The sampled soils were relatively wet (see soil water content in Fig. 3e). The seasonal or temporary wet conditions in soils may have created suitable anaerobic microhabitats for DSR. In addition, some sulfate-reducing microorganisms (e.g., *Desulfovibrio*-related strains) are not obligate anaerobic bacteria; reports indicate that they are able to survive in oxidizing environments (e.g., Marschall et al., 1993; Teske et al., 1996; Jonkers et al., 2005). These conditions imply that DSR could occur even in oxidizing microhabitats in soils, albeit at a small reaction rate. Moreover, some sulfate-reducing microorganisms were able to establish anaerobic microhabitats by different means, such as the formation of metallic sulfide aggregates (Fukui and Takii, 1990; Furusaka et al., 1991). These aggregates are likely to form around particles of organic compounds where oxygen could locally be removed rapidly because of the high respiration rates (Wind and Conrad, 1995). In the wet soils of southwestern karst areas in China, the decaying root and plant debris can provide such surroundings that make the occurrence of DSR reasonable.

In soils, TRS may result from bedrock weathering in addition to DSR activities. Compared with a typical anaerobic environment, the magnitude of isotope fractionation between SO_4^{2-} and TRS ($\Delta\delta^{34}S_{SO_4^{2-}-TRS}$) during DSR in the studied soils was small (<7‰) (Brunner and Bernasconi, 2005). Similarly, in the fen site Schlöppnerbrunnen of a forested catchment in northeastern Bavaria, Germany, the $\Delta\delta^{34}S_{SO_4^{2-}-TRS}$ values were approximately 3.5 and 2.1‰ at soil depths of 5 and 25 cm, respectively (Alewell and Novák, 2001). These observations of small values of $\Delta\delta^{34}S_{SO_4^{2-}-TRS}$ during DSR indicate that some

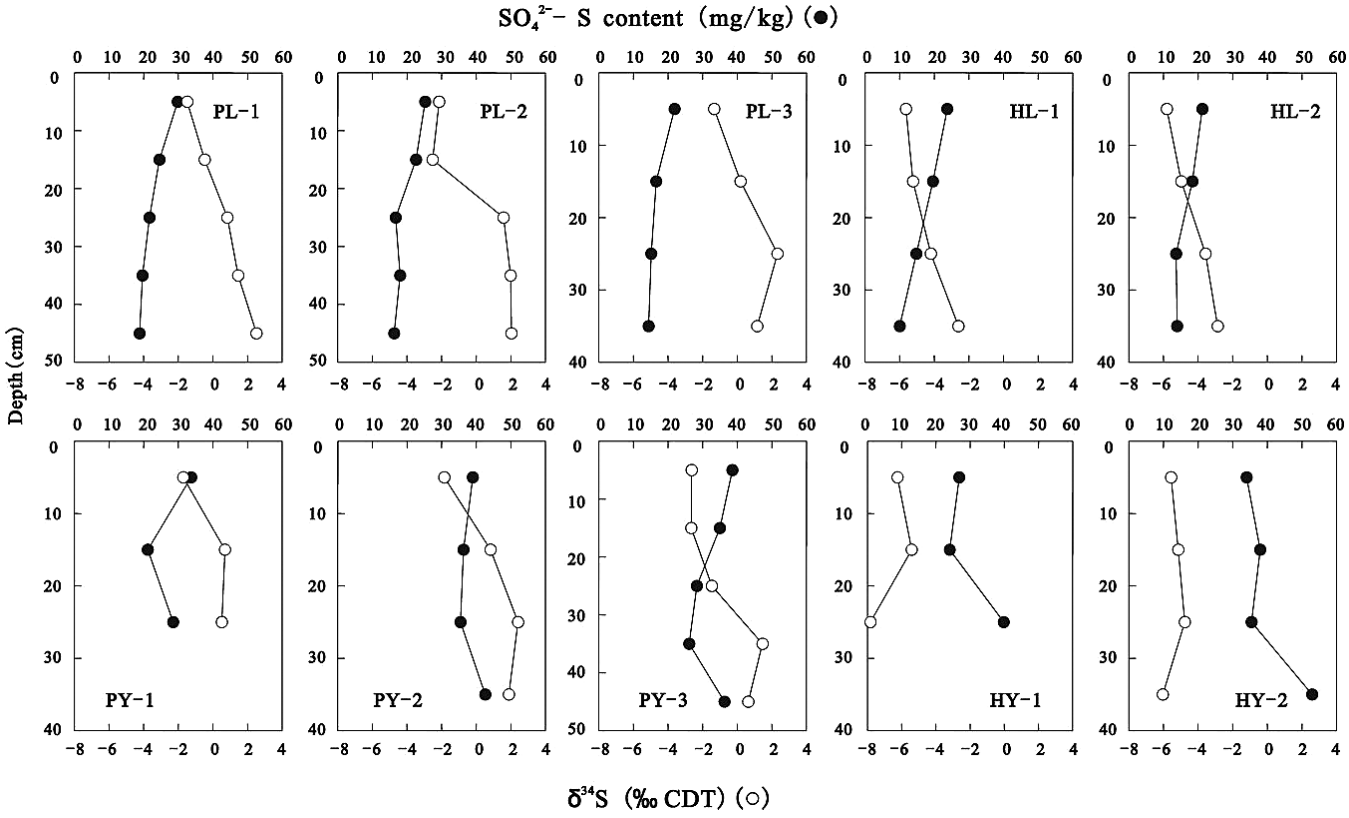

Fig. 7. Changes in S contents and $\delta^{34}S$ values of SO_4^{2-}–S with depth in soil profiles. CDT, Canyon Diablo Troilite; HL, limestone soil in Huanjiang; HY, yellow soil in Huanjiang; PL, limestone soil in Puding; PY, yellow soil in Puding.

sulfide S enriched in ^{34}S may have contributed to the increasing $\delta^{34}S$ values of TRS extracted in the studied soils. No mining activities are conducted in the studied sites. The $\delta^{34}S$ values of carbonate bedrock S were 12.3 ± 1.6‰ (mean ± SD; $n = 6$) in the Puding site and 15.6 ± 1.5‰ in the Huanjiang site. Considering the positive $\delta^{34}S$ values of carbonate bedrock S and the small values of $\Delta\delta^{34}S_{SO_4^{2-}-TRS}$, carbonate bedrock weathering could be a potential source of TRS in the studied soils. Other factors, such as the community structure of the sulfate-reducing microorganisms involved, the nature and availability of organic substrates, and the reaction rate of DSR in soils, may affect the distributions of $\Delta\delta^{34}S_{SO_4^{2-}-TRS}$ values during DSR (Hoek and Canfield, 2008 and references therein).

Generally, the remarkable depletion in ^{34}S of TRS relative to SO_4^{2-} and the parallel increase in $\delta^{34}S$ values of TRS and SO_4^{2-} indicate the occurrence of a bacterial reduction process of SO_4^{2-} in both soils. However, the vertical profiles of TRS contents in limestone soil were different from those in yellow soil (Fig. 4 and 8). The TRS contents increased with depth and reached the highest values at depths close to the bottom layers in the limestone soil profiles; the highest TRS content was observed on the subsurface layers, and TRS contents decreased below the subsurface layers in the yellow soil profiles. This result indicates that active DSR occurred at different depths in limestone soil and yellow soil. A relatively high TRS content in yellow soil was expected because the soil formation process of this type of soil is enrichment with pedogenic Fe and Al minerals (Liu, 2009). The deposition and subsequent leaching of SO_4^{2-} resulted in acid-induced dissolution of Fe minerals (Prietzel et al., 2004). This phenomenon may result in relatively high TRS content during DSR in yellow soil. The organic C contents decreased with depth (Fig. 3a), which could have led to the decreasing rate of DSR and the decrease in TRS contents at the bottom layers of the limestone soil and yellow soil profiles (Hao et al., 1996; Castro et al., 2000).

Transport and Accumulation of Sulfate

After the assimilation of SO_4^{2-} to form organic S compounds, the DSR reactions, adsorption, desorption, and leaching of SO_4^{2-} become important soil processes that can affect SO_4^{2-}–S distributions in the soil profiles. At both sites, decreasing SO_4^{2-}–S contents and increasing $\delta^{34}S$ values of SO_4^{2-}–S with depth were observed in the limestone soil profiles; the same trend was observed at depths from the surface layers to the middle layers in the yellow soil profiles (Fig. 7). From the middle layers to the bottom layers in the yellow soil profiles, the SO_4^{2-}–S contents increased, and the $\delta^{34}S$ values of SO_4^{2-}–S sharply decreased. As mentioned previously, DSR reactions could occur in both soils. Previous studies have demonstrated that the adsorption and desorption of SO_4^{2-} exhibit no significant S isotope fractionation (e.g., van Stempvoort et al., 1990). Therefore, the different depth distributions of SO_4^{2-}–S contents and the $\delta^{34}S$ values of SO_4^{2-}–S can be explained by the differences in the transport and subsequent accumulation of SO_4^{2-}, which in turn may be related to adsorption, desorption, and leaching of SO_4^{2-} in the studied soils.

In most soil environments, the adsorption and desorption of SO_4^{2-} are basically pH-dependent processes (Prietzel et al., 2004). The high pH values in limestone soil effectively prevented SO_4^{2-} adsorption; hence, the amount of adsorbed SO_4^{2-} was negligible in limestone soil. The residual SO_4^{2-} after biological S retention and secondary SO_4^{2-} (from the hydrolyzation of

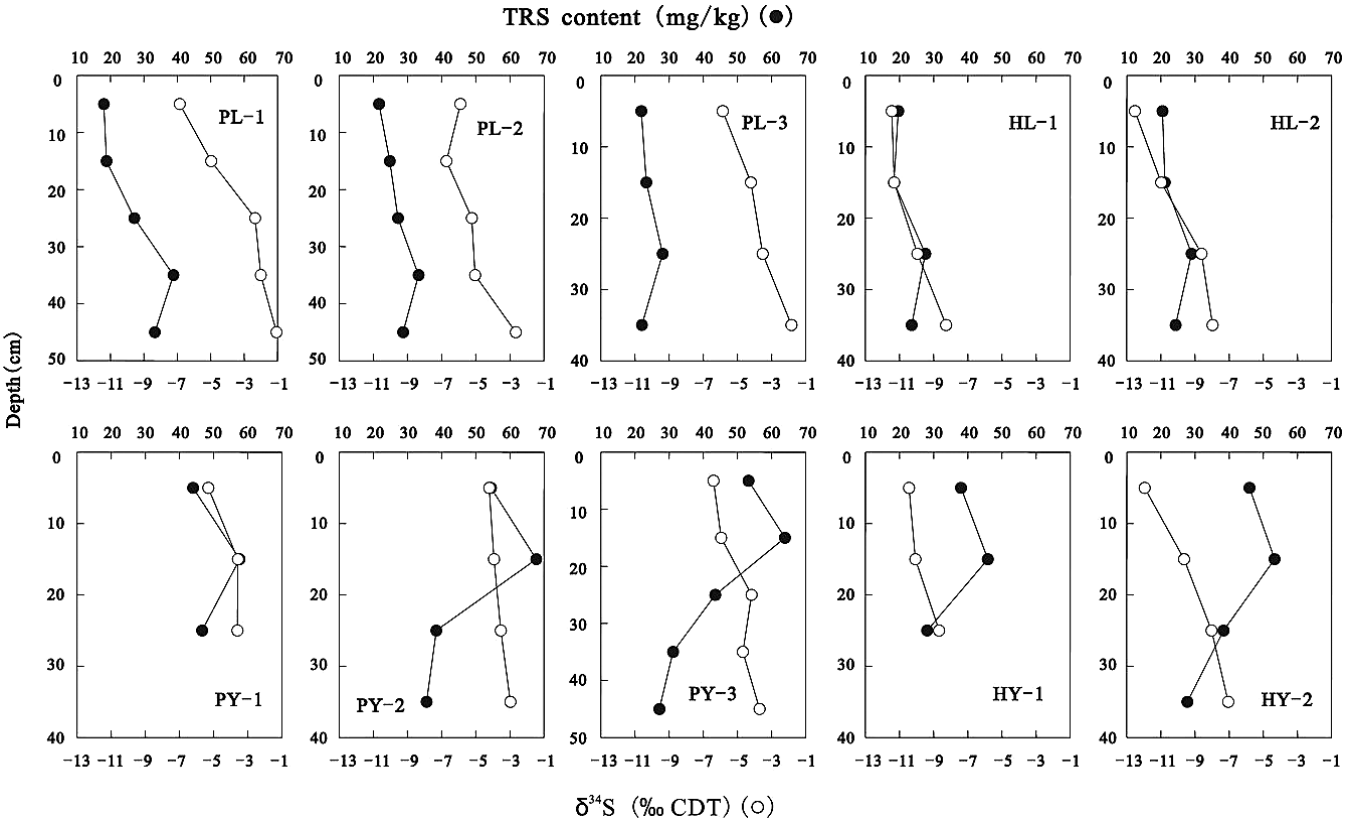

Fig. 8. Changes in S contents and $\delta^{34}S$ values of total reduced inorganic S (TRS) with depth in soil profiles. CDT, Canyon Diablo Troilite; HL, limestone soil in Huanjiang; HY, yellow soil in Huanjiang; PL, limestone soil in Puding; PY, yellow soil in Puding.

organic sulfate) are transported by leaching through the subsoil into groundwater or are lost by runoff on slopes. DSR and leaching of SO_4^{2-} decreased the SO_4^{2-}–S contents, whereas the $\delta^{34}S$ values of SO_4^{2-}–S increased with depth in the limestone soil profiles (Fig. 4 and 7).

In the surface layers of the yellow soil profiles, residual SO_4^{2-} after biological S retention and secondary SO_4^{2-} are adsorbed onto clay minerals (mainly hydrated silicate of magnesium and aluminum) or pedogenic Fe and Al oxohydroxides because of low pH values (Prietzel et al., 2004). This process mobilizes an equivalent amount of previously adsorbed SO_4^{2-}; this SO_4^{2-} is then leached with soil water in yellow soil. DSR and leaching of SO_4^{2-} from the surface layer to the middle layers of the yellow soil profiles decreased the SO_4^{2-}–S contents and increased the $\delta^{34}S$ values of SO_4^{2-}–S with depth (Fig. 4 and 7). Under acid deposition conditions, the increasing depth caused the continuous deposition and transport of SO_4^{2-} to lower the soil pH values further (Fig. 3c). Meanwhile, clay contents increased in the yellow soil profiles (Fig. 3d). This increase resulted in the increased SO_4^{2-} adsorption capacity of deep soil layers (Stanko-Golden et al., 1994; Prietzel et al., 2004). Thus, most of the transported SO_4^{2-} with lower $\delta^{34}S$ values than the residual SO_4^{2-} after in situ DSR can be re-adsorbed into the deep soil layers. This process increased the SO_4^{2-}–S contents and decreased the $\delta^{34}S$ values of SO_4^{2-}–S at the bottom layers of the yellow soil profiles (Fig. 4 and 7).

Different Acidification Stages of Limestone Soil and Yellow Soil

Analyses of the vertical profiles of SO_4^{2-}–S contents, $\delta^{34}S$ values of SO_4^{2-}–S, pH values, and clay contents indicate that limestone soil and yellow soil belong to different acidification stages according to the three-stage theory of mineral soil acidification proposed by Prietzel et al. (2004). The entire limestone soil profile could belong to the first stage because of high pH values and low clay contents (Fig. 3c and 3d). These conditions effectively prevented SO_4^{2-} adsorption into soil. The downward transport of SO_4^{2-} by leaching gradually depleted the basic cation pools from limestone soil. However, SO_4^{2-} transport did not decrease the pH values of limestone soil probably because of the abundant calcium and magnesium contents in limestone soil (Larssen et al., 2011).

The surface to middle layers (~20 cm deep) in the yellow soil profiles probably belong to the third acidification stage. At these depths, the residual SO_4^{2-} after the biological retention of SO_4^{2-} is adsorbed onto clay minerals or some pedogenic Fe and Al minerals because of the low pH values (Fig. 3c and 3d). The continuing input of SO_4^{2-} and H^+ from acid deposition resulted in remobilization of the previously adsorbed SO_4^{2-} (Prietzel et al., 2004). The desorbed SO_4^{2-} and secondary SO_4^{2-} from organic S mineralization may have transported downward. This process gradually decreased the soil pH values and caused a concomitant depletion of the soil base cation pool.

Yellow soil profiles with depths below 20 cm belong to the second acidification stage. The elevated H^+ concentration in the soil solution and increased clay contents induces an increasing adsorption of SO_4^{2-} at depths below 20 cm in the yellow soil profiles (Fig. 3d). The transported SO_4^{2-} is re-adsorbed and accumulates at deep layers in the yellow soil profiles (Fig. 4 and 7). The adsorption and accumulation of SO_4^{2-} at the bottom layers reduced the downward flux of SO_4^{2-} and H^+

and consequently decelerated basic cation depletion and soil acidification in yellow soil.

Conclusions

The S contents and the $\delta^{34}S$ values of total S, organic S, SO_4^{2-}–S, and TRS differ in limestone soil and yellow soil under similar acid deposition conditions. This result is attributed to the different processes of S retention and cycling in the two soils. This condition is closely related to the respective physical–chemical properties of limestone soil and yellow soil. Most of the deposited SO_4^{2-} was mainly retained as organic S in both soils; the extents of organic S mineralization and transport of organic sulfate were different. This difference explains the different vertical profiles of total S and organic S contents in limestone soil and yellow soil. The remarkable depletion in ^{34}S of TRS relative to SO_4^{2-} and the parallel increasing $\delta^{34}S$ values of TRS and SO_4^{2-} indicate that, after the formation of organic S, the deposited SO_4^{2-} underwent the DSR reaction to form TRS in both soils. The high pH values inhibited SO_4^{2-} adsorption in limestone soil. Most of the residual SO_4^{2-} after biological S retention and secondary SO_4^{2-} from organic sulfate hydrolyzation in limestone soil were lost by leaching. The deposited SO_4^{2-} was first transformed into organic S and TRS by biological S retention and then adsorbed into yellow soil because of the low pH values. The continuing input of SO_4^{2-} from acid deposition resulted in the remobilization of previously adsorbed SO_4^{2-}; the desorbed SO_4^{2-} and secondary SO_4^{2-} can be transported downward in the yellow soil profiles. Under S deposition conditions, the transport of SO_4^{2-} lowered the pH values of the deep soil layers; clay contents increased with depth in the yellow soil profiles and resulted in the increased SO_4^{2-} adsorption capacity of the deep soil layers of the yellow soil. The transported SO_4^{2-} was readsorbed and accumulated at the bottom layers of the yellow soil profiles. In addition to biological S retention to form organic S and TRS, SO_4^{2-} adsorption was another important S retention process for deposited S in the yellow soil. This process explains the higher SO_4^{2-}–S contents in yellow soil than in limestone soil.

The limestone soil profiles may belong to the first acidification stage. The surface to middle layers of the yellow soil profiles may belong to the third acidification stage. Layers below the middle layers of the yellow soil profiles may belong to the second acidification stage. The effects of acid deposition on yellow soil were more serious compared with those on limestone soil. This difference is caused by the considerable accumulation of atmospherically deposited SO_4^{2-}, which may be adsorbed onto pedogenic Fe, Al, and clay minerals in yellow soil. The desorption and subsequent leaching of the adsorbed SO_4^{2-} under acid deposition can result in soil acidification and accelerate the loss of basic cations from yellow soil. However, a greater amount of deposited S was retained as organic S in limestone soil compared with yellow soil. Sulfate adsorption was negligible in limestone soil. Therefore, limestone soil may release more S into river water through organic S mineralization for a fairly long period after the considerable drop in the annual S deposition rate. This process could occur when rigorous environmental protection policies are introduced and a highly effective technology for desulfurization is applied for coal-fired power plants in China. Studies on the effects on soil and river ecosystems in southwestern areas of China are expected in the future.

Acknowledgments

This work was supported by Ministry of Science and Technology of China through the National Basic Research Program of China ("973" Program, Grant No: 2013CB956401) and the National Natural Science Foundation of China (No. 41103048, 41130536, 41073096). The authors thank two anonymous reviewers for helpful comments and suggestions that greatly improved the manuscript.

References

Alewell, C., and M. Gehre. 1999. Patterns of stable S isotopes in a forested catchment as indicators for biological S turnover. Biogeochemistry 47:319–333. doi:10.1007/BF00992912

Alewell, C., and M. Novák. 2001. Spotting zones of dissimilatory sulfate reduction in a forested catchment: The ^{34}S-^{35}S approach. Environ. Pollut. 112:369–377. doi:10.1016/S0269-7491(00)00137-8

APHA (American Public Health Association). 1998. Standard methods for the examination of water and wastewater. 20th ed. APHA, Washington, DC.

Backlund, K., Boman, A., Fröjdö, S., and M. Åström. 2005. An analytical procedure for determination of sulfur species and isotopes in boreal acid sulfate soils and sediments. Agric. Food Sci. 14:70–82. doi:10.2137/1459606054224147

Bates, A.L., E.C. Spiker, W.H. Orem, and W.C. Burnett. 1993. Speciation and isotopic composition of sulfur in sediments from Jellyfish Lake, Palau. Chem. Geol. 106:63–76. doi:10.1016/0009-2541(93)90166-G

Bollag, J.M., and G. Stotzky. 1990. Soil biochemistry. Marcel Dekker, New York.

Brunner, B., and S.M. Bernasconi. 2005. A revised isotope fractionation model for dissimilatory sulfate reduction in sulfate reducing bacteria. Geochim. Cosmochim. Acta 69:4759–4771. doi:10.1016/j.gca.2005.04.015

Castro, H.F., N.H. Wiliams, and A. Ogram. 2000. Phylogeny of sulfate-reducing bacteria. FEMS Microbiol. Ecol. 31:1–9.

Conway, A. 1978. Soil physical-chemical analysis. Technology Press, Shanghai.

Ding, H. 2010. Water and nutrients cycle of typical karst peak-cluster depression: A case study of Mulian catchment, north-west Guanxi Province, China. PhD thesis, Chinese Academy of Sciences, Shanghai, China. (In Chinese.)

Driscoll, C.T., K.M. Driscoll, M.J. Mitchell, and D.J. Raynal. 2003. Effects of acidic deposition on forest and aquatic ecosystems in New York State. Environ. Pollut. 123:327–336. doi:10.1016/S0269-7491(03)00019-8

Driscoll, C.T., G.E. Likens, and M.R. Church. 1998. Recovery of soil and surface waters in the northeastern US, from decreases in atmospheric deposition of sulfur. Water Air Soil Pollut. 105:319–329. doi:10.1023/A:1005008315977

Fossing, H., and B.B. Jørgensen. 1989. Measurement of bacterial sulfate reduction in sediments: Evaluation of a single-step chromium reduction method. Biogeochemistry 8:205–222. doi:10.1007/BF00002889

Fukui, M., and S. Takii. 1990. Survival of sulfate-reducing bacteria in oxic surface sediment of a seawater lake. FEMS Microbiol. Lett. 73:317–322. doi:10.1111/j.1574-6968.1990.tb03955.x

Furusaka, C., N. Nagatsuka, and S. Ishikuri. 1991. Survival of sulfate reducing bacteria in oxic layers of paddy soils. In: J. Berthelin, editor, Developments in geochemistry. Elsevier, Amsterdam. p. 259–264.

Gebauer, G., A. Giesemann, E.D. Schulze, and H.J. Jäger. 1994. Isotope ratios and concentrations of sulfur and nitrogen in needles and soils of Piceaabies stands as influenced by atmospheric deposition of sulfur and nitrogen compounds. Plant Soil 164:267–281. doi:10.1007/BF00010079

Giesemann, A., H.J. Jager, A.L. Norman, H.R. Krouse, and W.A. Brand. 1994. On-line sulphur isotope determination using an elemental analyzer coupled to a mass spectrometer. Anal. Chem. 66:2816–2819. doi:10.1021/ac00090a005

Hall, G.E.M., J.-C. Pelchat, and J. Loop. 1988. Separation and recovery of various sulphur species in sedimentary rocks for stable sulphur isotopic determination. Chem. Geol. 67:35–45. doi:10.1016/0009-2541(88)90004-6

Han, G.L., and C.Q. Liu. 2004. Water geochemistry controlled by carbonate dissolution: A study of the river waters draining karst-dominated terrain, Guizhou Province. Chem. Geol. 204:1–21. doi:10.1016/j.chemgeo.2003.09.009

Hao, O.J., J.M. Chen, L. Huang, and R.L. Buglass. 1996. Sulfate-reducing bacteria. Crit. Rev. Environ. Sci. Technol. 26:155–187. doi:10.1080/10643389609388489

Hoek, J., and D.E. Canfield. 2008. Controls on isotope fractionation during dissimilatory sulfate reduction. In: C., Dahl and C.G. Friedrich, editors, Microbial sulfur metabolism. Springer, Berlin, Heidelberg, New York. p. 273–283.

Jonkers, H.M., I.O. Koh, P. Behrend, G. Muyzer, and D. de Beer. 2005. Aerobic organic carbon mineralization by sulfate-reducing bacteria in the oxygen-saturated photic zone of a hypersaline microbial mat. Microb. Ecol. 49:291–300. doi:10.1007/s00248-004-0260-y

Kirchner, J.W., and E. Lydersen. 1995. Base cation depletion and potential long-term acidiðcation of Norwegian catchments. Environ. Sci. Technol. 29:1953–1960. doi:10.1021/es00008a012

Krouse, H.R., and V.A. Grinenko. 1991. Stable isotopes: Natural and anthropogenic sulphur in the environment. SCOPE 43. John Wiley & Sons, Chichester, UK.

Larssen, T., L. Duan, and J. Mulder. 2011. Deposition and leaching of sulfur, nitrogen and calcium in four forested catchments in China: Implications for acidification. Environ. Sci. Technol. 45:1192–1198. doi:10.1021/es103426p

Larssen, T., E. Lydersen, D. Tang, Y. He, J.X. Gao, H.Y. Liu, H.M. Seip, R.D. Vogt, J. Mulder, M. Shao, Y.H. Wang, H. Shang, X.S. Zhang, S. Solberg, W. Aas, T. Økland, O. Eilertsen, V. Angell, Q.R. Liu, D.W. Zhao, R.J. Xiang, J.S. Xiao, and J.H. Luo. 2006. Acid rain in China. Environ. Sci. Technol. 40:418–425. doi:10.1021/es0626133

Larssen, T., H.M. Seip, A. Semb, J. Mulder, I.P. Muniz, R.D. Vogt, E. Lydersen, V. Angell, D. Tang, and O. Eilertsen. 1999. Acid deposition and its effects in China: An overview. Environ. Sci. Policy 2:9–24. doi:10.1016/S1462-9011(98)00043-4

Larssen, T., J.L. Xiong, R.D. Vogt, H.M. Seip, B.H. Liao, and D.W. Zhao. 1998. Studies of soils, soil water and stream water at a small catchment near Guiyang, China. Water Air Soil Pollut. 101:137–162. doi:10.1023/A:1004985209931

Lavelle, P., and A.V. Spain. 2003. Soil ecology. Kluwer Academic, New York.

Li, L., T. Liu, X. Li, W.J. Liu, and C.Q. Liu. 2012. Vertical distribution patterns of organic carbon and its isotopic composition in typical soil types in Guizhou karst areas of Southwest China. Chin. J. Ecol. 31:241–247. (In Chinese.)

Li, S.L., D. Calmels, G.L. Han, J. Gaillardet, and C.Q. Liu. 2008. Sulfuric acid as an agent of carbonate weathering constrained by δ^{13}XΔIX: Εξαμπλεσ φρομ Σουτηωεστ Χηινα. Earth Planet. Sci. Lett. 270:189–199. doi:10.1016/j.epsl.2008.02.039

Likens, G.E., C.T. Driscoll, D.C. Buso, M.J. Mitchell, G.M. Lovett, S.W. Bailey, T.G. Siccama, W.A. Reiners, and C. Alewell. 2002. The biogeochemistry of sulfur at Hubbard Brook. Biogeochemistry 60:235–316. doi:10.1023/A:1020972100496

Liu, C.-Q. 2009. Biogeochemical processes and cycling of nutrients in the earth's surface: Cycling of nutrients in soil-plant systems of karstic environments, southwest China. Science Press, Beijing. (In Chinese.)

Marschall, C., P. Frenzel, and H. Cypionka. 1993. Influence of oxygen on sulfate reduction and growth of sulfate-reducing bacteria. Arch. Microbiol. 159:168–173. doi:10.1007/BF00250278

Mayer, B., K.-H. Feger, A. Giesemann, and H.-J. Jäger. 1995a. Interpretation of sulfur cycling in two catchments in the Black Forest (Germany) using stable sulfur and oxygen isotope data. Biogeochemistry 30:31–58. doi:10.1007/BF02181039

Mayer, B., P. Fritz, J. Pritezel, and H.R. Krouse. 1995b. The use of stable sulphur and oxygen isotope ratios for interpreting the mobility of sulfate in aerobic forest soils. Appl. Geochem. 10:161–173. doi:10.1016/0883-2927(94)00054-A

Midwood, A.J., and T.W. Boutton. 1998. Soil carbonate decomposition by acid has little effect on δ^{13}X οφ οργανιχ ματτερ. Soil Biol. Biochem. 30:1301–1307. doi:10.1016/S0038-0717(98)00030-3

Mitchell, M.J., M.B. David, and R.B. Harrison. 1992. Sulfur dynamics of forest ecosystems. In: R.W., Howarth, J.W.B. Stewart, and M.V. Ivanov, editors, Sulfur cycling on the continents, wetlands, terrestrial ecosystems, and associated water bodies, scientific committee on problems of the environment SCOPE 48. John Wiley & Sons, Chichester, UK. p. 215–254.

Mitchell, M.J., B. Mayer, S.W. Bailey, J.W. Hornbeck, C. Alewell, C.T. Driscoll, and G.E. Linken. 2001. Use of stable isotope ratios for evaluating sulfur sources and losses at the Hubbard Brook Experimental Forest. Water Air Soil Pollut. 130:75–86. doi:10.1023/A:1012295301541

Mitchell, M.J., D.J. Raynal, and C.T. Driscoll. 1996. Biogeochemistry of a forested watershed in the central Adirondack Mountains: Temporal changes and mass balances. Water Air Soil Pollut. 88:355–369. doi:10.1007/BF00294111

Mörth, C.M., P. Torssander, O.J. Kjønnas, A.O. Stunaes, F. Moldan, and R. Giesler. 2005. Mineralization of organic sulfur delays recovery from anthropogenic acidification. Environ. Sci. Technol. 39:5234–5240. doi:10.1021/es048169q

Norman, A.L., A. Giesemann, H.R. Krouse, and H.J. Jäger. 2002. Sulphur isotope fractionation during sulphur mineralization: Results of an incubation-extraction experiment with a Black Forest soil. Soil Biol. Biochem. 34:1425–1438. doi:10.1016/S0038-0717(02)00086-X

Novák, M., S.H. Bottrell, and E. Prechova. 2001. Sulfur isotope inventories of atmospheric deposition, spruce forest floor and living Sphagnum along a NW-SE transect across Europe. Biogeochemistry 53:23–50. doi:10.1023/A:1010792205756

Novák, M., F. Buzek, A.F. Harrison, E. Přechová, I. Jäckvoá, and D. Fottová. 2003. Similarity between C, N and S stable isotope proðles in European spruce forest soils: Implications for the use of δ^{34}Σ ασ α τραχερ. Appl. Geochem. 18:765–779. doi:10.1016/S0883-2927(02)00162-2

Novák, M., J.W. Kirchner, D. Fottova, E. Přechová, I. Jäckvoá, P. Krám, and J. Hruška. 2005. Isotopic evidence for processes of sulfur retention/release in 13 forested catchments spanning a strong pollution gradient (Czech Republic, central Europe). Global Biogeochem. Cycles 19:GB4012. doi:10.1029/2004GB002396

Novák, M., J.W. Kirchner, H. Groscheova, M. Havel, J. Černý, R. Krejčí, and F. Buzek. 2000. Sulfur isotope dynamics in two central European watersheds affected by high atmospheric deposition of SOx. Geochim. Cosmochim. Acta 64:367–383. doi:10.1016/S0016-7037(99)00298-7

Novák, M., R.K. Wieder, and W.R. Schell. 1994. Sulfur during early diagenesis in Sphagnum peat: Insights from δ^{34}Σ ρατιο προφιλεσ ιν 2λ0Πβ−δατεδ πεατ χορεσ. Limnol. Oceanogr. 39:1172–1185. doi:10.4319/lo.1994.39.5.1172

Novák, M., S.H. Bottrell, D. Fottová, F. Buzek, H. Groscheová, and K. Zák. 1996. Sulfur isotopic signals in forest soils of central Europe along an air pollution gradient. Environ. Sci. Technol. 30:3473–3476. doi:10.1021/es960106n

Prietzel, J., B. Mayer, H.R. Krouse, K.E. Rehfuess, and P. Fritz. 1995. Transformation of simulated wet sulfate deposition in forest soils assessed by a core experiment using stable sulfur isotopes. Water Air Soil Pollut. 79:243–260. doi:10.1007/BF01100440

Prietzel, J., B. Mayer, and A.H. Legge. 2004. Cumulative impact of 40 years of industrial sulfur emissions on a forest soil in west-central Alberta (Canada). Environ. Pollut. 132:129–144. doi:10.1016/j.envpol.2004.03.016

Schoenau, J.J., and J.R. Bettany. 1987. Organic matter leaching as a component of carbon, nitrogen, phosphorus, and sulfur cycles in a forest, grassland, and gleyed soil. Soil Sci. Soc. Am. J. 51:646–651. doi:10.2136/sssaj1987.03615995005100030017x

Seip, H.M., D.W. Zhao, J.L. Xiong, D.W. Zhao, T. Larssen, B.H. Liao, and R.D. Vogt. 1995. Acid deposition and its effects in southwestern China. Water Air Soil Pollut. 85:2301–2306. doi:10.1007/BF01186177

Stanko-Golden, K.M., W.T. Swank, and J.W. Fitzgerald. 1994. Factors affecting sulfate adsorption, organic sulfur formation, and mobilization in forest and grassland spodosols. Biol. Fertil. Soils 17:289–296. doi:10.1007/BF00383984

Stevenson, F.J., and M.A. Cole. 1999. Cycles of soil: Carbon, nitrogen, phosphorus, sulfur, micronutrients. 2nd ed. John Wiley & Sons, New York.

Tan, Z., R.G. McLaren, and K.C. Cameron. 1994. Forms of sulfur extracted from field moist, air-dried and conditional soils. Aust. J. Soil Res. 32:823–834. doi:10.1071/SR9940823

Teske, A., C. Wawer, G. Muyzer, and N.B. Ramsing. 1996. Distribution of sulfate-reducing bacteria in a Stratiðed Fjord (Mariager Fjord, Denmark) as evaluated by most-probable-number counts and denaturing gradient gel electrophoresis of PCR-ampliðed ribosomal DNA fragments. Appl. Environ. Microbiol. 62:1405–1415.

Tuttle, M.L., A.C. Rice, and M.B. Goldhaber. 1990. Geochemistry of organic and inorganic sulfur in ancient and modern lacustrine environments: Case studies of fresh-water and saline lakes. In: W. L. Orr and C. M. White, editors, Geochemistry of sulfur in fossil fuels. ACS Symp. Series. Am. Chem. Soc., Washington, DC. p. 114–148.

Van Stempvoort, D.R., E.J. Reardon, and P. Fritz. 1990. Fractionation of sulfur and oxygen isotopes in sulfate by soil sorption. Geochim. Cosmochim. Acta 54:2817–2826. doi:10.1016/0016-7037(90)90016-E

Wang, Z.Y., X.S. Zhang, Y. Zhang, Z. Wang, and J. Mulder. 2011. Accumulation of different sulfur fractions in Chinese forest soil under acid deposition. J. Environ. Monit. 13:2463–2470. doi:10.1039/c1em10313j

Wind, T., and R. Conrad. 1995. Sulfur compounds, potential turnover of sulfate and thiosulfate, and numbers of sulfate-reducing bacteria in planted and unplanted paddy soil. FEMS Microbiol. Ecol. 18:257–266. doi:10.1111/j.1574-6941.1995.tb00182.x

Xu, Z.F., and C.Q. Liu. 2007. Chemical weathering in the upper reaches of Xijiang River draining the Yunnan-Guizhou Plateau, Southwest China. Chem. Geol. 239:83–95. doi:10.1016/j.chemgeo.2006.12.008

Zhang, Y.L. 2008. Low molecular weight carboxylc acids in precipitation,in the rural area of Anshun,West Guizhou Province:Comparison with acid precipitation in other areas of Guizhou,China. PhD thesis, Chinese Academy of Sciences, Shanghai, China. (In Chinese.)

Zhao, D.W., T. Larssen, D.B. Zhang, S.D. Gao, R.D. Vogt, H.M. Seip, and O.J. Lund. 2001. Acid deposition and acidification of soil and water in the Tie Shan Ping area, Chongqing, China. Water Air Soil Pollut. 130:1733–1738. doi:10.1023/A:1013999701234

Zhao, D.W., H.M. Seip, D. Zhao, and D. Zhang. 1994. Pattern and cause of acidic deposition in Chongqing region, Sichuan Province, China. Water Air Soil Pollut. 77:27–48.

Zhao, D., and B. Sun. 1986. Air pollution and acid rain in China. Ambio 15:2–5.

Zhao, D., J. Xiong, Y. Xu, and W.H. Chan. 1988. Acid rain in southwestern China. Atmos. Environ. 22:349–358. doi:10.1016/0004-6981(88)90040-6

Zhao, F.Z., J.S. Knights, Z.Y. Hu, and S.p. McGrath. 2003. Stable sulfur isotope ratios indicates long-term changes in sulfur deposition in the broadbalk experiments since 1845. J. Environ. Qual. 32:33–39. doi:10.2134/jeq2003.3300

Zhou, W., S.T. Li, H. Wang, P. He, and B. Lin. 1999. Mineralization of organic sulfur and its importance as a reservoir plant-available sulfur in upland soils of north China. Biol. Fertil. Soils 30:245–250. doi:10.1007/s003740050615

Zhu, S.F., and C.-Q. Liu. 2006. Vertical patterns of stable carbon isotope in soils and particle-size fractions of karst areas, Southwest China. Environ. Geol. 50:1119–1127. doi:10.1007/s00254-006-0285-2